# Seismic modelling and imaging for a shallow $CO_2$ injection project

*Davood Nowroozi, Donald C. Lawton and Hassan Khaniani*

*CREWES Project, University of Calgary, and CMC Research Institutes, Inc.*

## Summary

We investigate the effects of $CO_2$ storage monitoring with seismic imaging using fluid simulation, rock physics and wavefield propagation. The fluid simulation is used to estimate the saturation of $CO_2$ and reservoir pressure. The influence of saturated $CO_2$ on rock elastic properties are approximated using Gassmann's equation. Using a numerical example, we show $CO_2$ flow simulation plume create the Gaussian shaped varition of the elastic properties around $CO_2$ injection point. The result of wave propagation and reverse time migration for a time-lapse study are compared with a scatterpoint method which has non-Gaussian shaped (i.e. a sharp contrast). The results shows that the amplitude of forward modeling and RTM image of injection zone is smaller compared to the scatter point models. This suggests the use of alternative approach such as traveltime variation as compared to reflection imaging.

## Introduction

The Field Research Station (FRS) is a project developed by CMC Research Institute Inc and the University of Calgary. The project area covers 1 km *1 km and is located in southern Alberta, Canada (Figure 1). The research plan is to inject a very controlled and limited amount of $CO_2$ in the shallow layers to monitor migration and behavior of gas plume by seismic and other methods. This project plans to inject constant mass of up to 1000 ton/year of $CO_2$ in the target zones for five years.

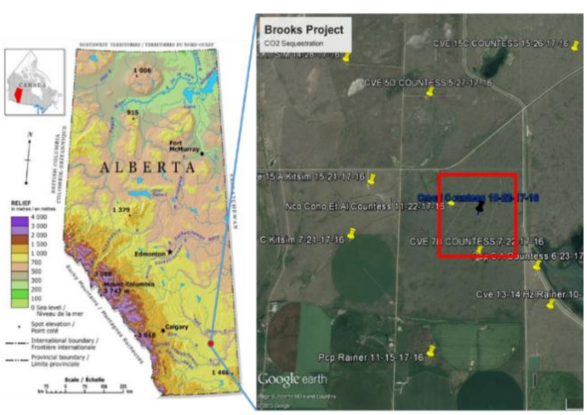


FIG.1. Project location map.

The research steps was defined in Figure 2. The objective of this study is to find an optimum framework for using the waveform information in terms of traveltime and amplitude for CO2 injection projects. The seismic time lapse data acquisition and processing are designed based on the wavefield propagation model. For evaluation of the boundaries of CO2 injection, the data obtained from different acquisition configurations such as surface seismic, Vertical Seismic Profile (VSP), and cross well tomography are compared.

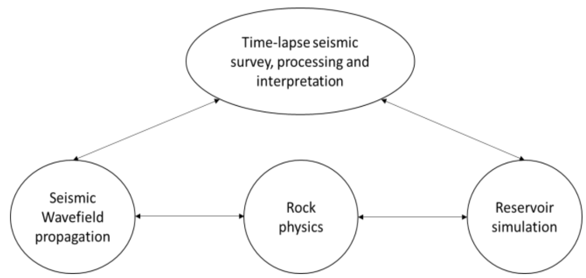


FIG.2: The reservoir characterization process

During the $CO_2$ injection in the target layer (297 to 302 m depth), dynamic parameters of the reservoir, such as pressure and saturation, changes. These changes influence the seismic response through moduli and from fluid substitution models.

Time-lapse seismic analysis of reservoir was assessed by seismic finite-difference time domain (FDTD) modeling based on an acoustic velocity-stress staggered leapfrog scheme. The FDTD is 2nd order in time and 4th order in space on a central finite difference (CFD) approach. As a result of $CO_2$ substitution, there is a velocity reduction in the reservoir, leading to a time delay seismic events below the injected plume and also a small change in the amplitude of reservoir reflections. The seismic synthetic modeling and RTM analysis shows that seismic travel-time monitoring can be an effective method to monitor the $CO_2$ injection compared with monitoring of reflection amplitudes.

This paper is organized as follows: Firstly, a framework for making a geomodel of $CO_2$ injection is briefly described. Secondly, the $CO_2$ injection simulation result are presented amd thirdly, the reservoir model for the basline (before injection) and monitor conditions (after injection) are investigated using time-lapse analysis.

## Fluid simulation

The fluid simulation is based on diffusion equations that relate mass transfer's calculation and fluid flow models. Hydraulic diffusivity (see e.g., Shapiro and Dinske, 2009) is an essential part of diffusion equation. constructing the hydraulic diffusivity requires to acquire data from different disciplines, such as geological set and studies, seismic data, well log data and petrophysical interpretation.

The permeability and porosity are the base of a geomodel.For the permeability modeling, Timur-Coates (KTIM) and the Sclumberger-Doll-Research (KSDR) models from Nuclear Magnetic Resonance (NMR) log were available and KTIM was used for $K_x$ and $K_y$ modeling. Because of layering and sharp changes in the vertical permeability (perpendicular to the geological layers), $K_z$ was considered equal to 10% of KTIM. Also an average of the porosity logs was considered for geostatistical porosity model. The resulting geomodel was the base for fluid simulation and subsequent reservoir modelling (Figure. 4).

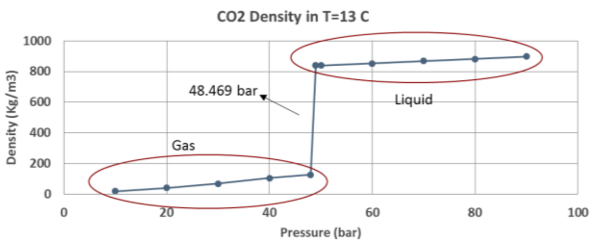


FIG.3. The phase behavior with the pressure change.

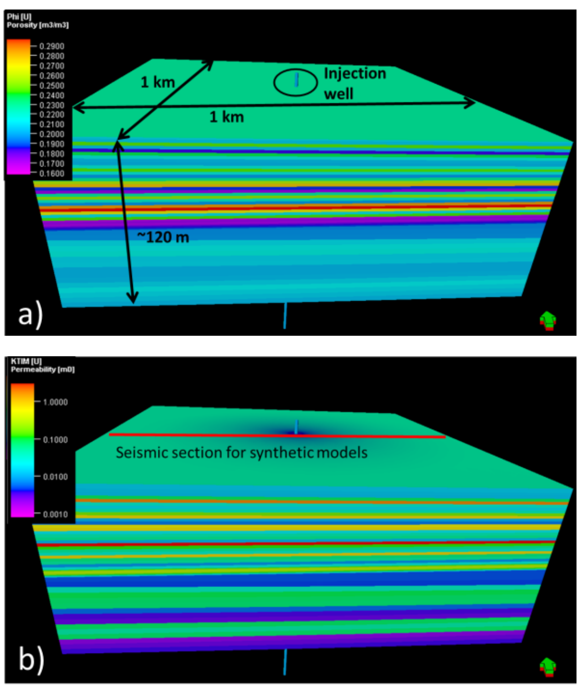


FIG.4. Geomodel for the porosity (a) and permeability (b).

The $CO_2$ saturation is related to trapping efficiency and the volume of irreducible water. For the low permeability area as the injection target in sandstone, trapping efficacy can be up to 65 percent (Bachu, 2013).

A Black Oil simulator was used for the fluid simulation with results shown in Figure 5. However, the simulation for selected injection strategy showed that saturation in the injection point may reach a maximum of 60% and the reservoir pressure may exceed the fracture pressure equal to 14 MPa. The numerical simulation led to the next part of the rock physics study and velocity/density/acoustic impedance calculation.Also during the injection, as Figure 3, a phase change happens in p=48.469 bar.

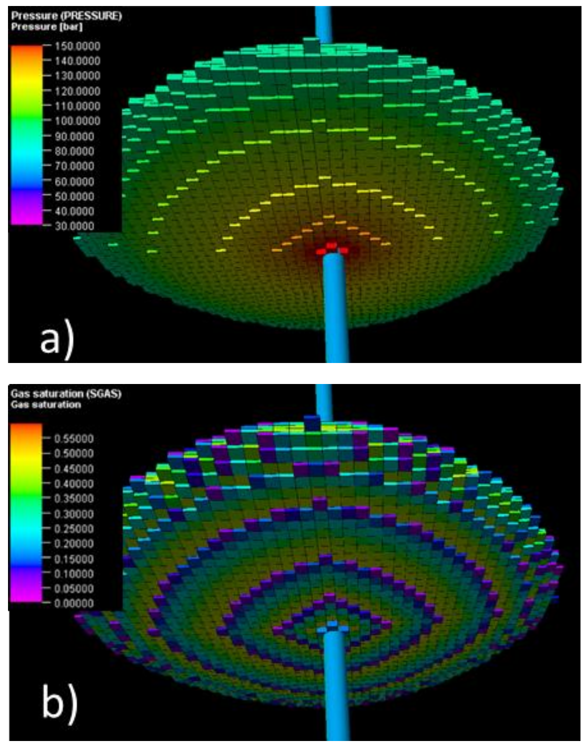


FIG.5. Reservoir simulation results. a) Pressure, b) $CO_2$ saturation

**Forward modeling strategy**

The 2D acoustic wave equation can be expressed by Euler's equation and the equation of continuity (e.g., Brekhovskikh, 1960 and Zakaria et al., 2000). A system of first-order differential equations in terms of the particle velocities and stresses can be found using,

$$\left.\begin{aligned} \frac{\partial u}{\partial t} &= -\frac{1}{\rho}\frac{\partial p}{\partial x}, \\ \frac{\partial v}{\partial t} &= -\frac{1}{\rho}\frac{\partial p}{\partial z}, \end{aligned}\right\} \qquad \textit{Euler} \qquad\qquad (1)$$

$$\frac{\partial p}{\partial t} = -\rho v_P{}^2 \left(\frac{\partial u}{\partial x} + \frac{\partial v}{\partial z}\right), \qquad \textit{Continuity}$$

where $p$ is the pressure, $u$ and $v$ are particle velocities in lateral $x$ and vertical $z$ directions respectively. The parameters $\rho$ and $v_P$ are density and P-wave velocity and $t$ is the time. The numerical solution is based on the FDTD of staggered grid in a leapfrog scheme. The FDTD is 2nd order in time and 4th order in space on Central Finite Difference (CFD). The Perfectly Matched Layers (PML) boundary condition of Zhou (2003) is used for all edge of the model except the surface. Displacement vectors in Equation (1) show that in order to characterize the acoustic wavefield, multicomponent acquisition and imaging are useful.

## Migration strategy

The RTM include three simultaneous imaging conditions given by,

$$I_u(\vec{x}) = \int_0^{T_{\max}} S_u(t,\vec{x}) r_u(t,\vec{x}) dt,$$
$$I_v(\vec{x}) = \int_0^{T_{\max}} S_v(t,\vec{x}) r_v(t,\vec{x}) dt, \qquad (2)$$
$$I_p(\vec{x}) = \int_0^{T_{\max}} S_p(t,\vec{x}) r_p(t,\vec{x}) dt,$$

Where, $I(\mathbf{x})$ is the migrated image in subsurface coordinate $\vec{\mathbf{x}} = (x,z)$, $T_{max}$ is maximum recorded time, $S(t,\vec{\mathbf{x}})$ is forward propagated source and $r(t,\vec{\mathbf{x}})$ is the backward propagated receivers. The subscripts $p$, $u$ and $v$ correspond to three images for pressure and displacements obtained by imaging conditions. Note that here Einstein summation convention is not used for repeated indices. The imaging condition of RTM algorithm is crosscorelation of forward propagationg sources and backward propagating recievers.

## Perturbation model and wave propagation

The $CO_2$ injection in the acquifer, decreases the bulk modulus, P wave velocity and bulk density and so the reflection coefficient and acoustic impedance. The change in velocity was estimated by the Gassmann's equation and for the 60% $CO_2$ saturation it results in a 4% reduction in P-wave velocity and this change was incorporated into the time-lapse model. To describe the effect of model perturbation as a result of $CO_2$ diffusion two numerical examples are performed. As shown in Figure 5 and 6.a, the change in pressure and saturation of $CO_2$ has Gaussian shaped distribution (i.e., smoothed gas plume). We assume that these changes have similar effect to the elastic properies of rock overtime such that they have smoothed perturbation. Using numerical examples, the effect of smoothed perturbation (or diffusive perturbation) in reflection and transmition of wavefield are compared with the regular scatterpoint models (i.e., with sharp contrast).

## Numerical example

As mentioned above, the first example is shown in Figure 6 that compares seismic responses of same perturbations in diffusive and regular scatterpoints in a simple three layer model (Figure 6a). A Ricker source wavelet (f=45 HZ) is injected in the updated model (Figure 6b).The subtraction of the base seismic model befor injection and after is calculated and it is shown in Fig.5.c and d for Uz and Ux components. The result of RTM on seismic differences for two components (Fig.6.e and f) show an image in the correct locations for the solid shapes. For the gas plume, the image is not clear and in the real situation, but the amplitude change and effect of time delay is recognizable (Figure.6e ,6f).

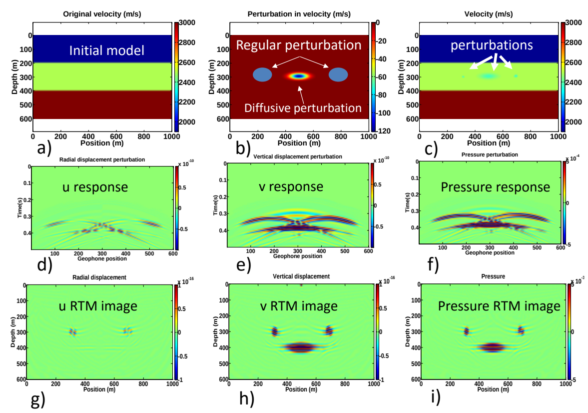


Figure.6. The result of seismic modeling for the velocity change in the solid block and the gas diffusive shape. The first row is a simple 3-layer model with velocity change as a solid block and diffusive perturbation in the mid layer. The second row shows seismic modeling for the pressure $p$ and $u$ (radial component) and $v$ (vertical component). The last row is the result of RTM on the seismic response (for $u$, $v$ and $p$ ).

Figure 7 shows the second example that shows a cake layers' model of p-wave velocity according to CMC well (the formations are flat in the area). The tested pattern is a cross well (as Figure 7) with a single shot and has 500 m long multicomponent geophones spread positioned inside the well. The receivers interval of dx=3 m and the source is positioned in nearby well with distance of 50 m from recievers. Figure 7b shows synthetic data for pressure component for the base model. The perturbed pressure of Figure 7c is migrated by RTM as displayed in Figure 7d. As shown in Figure 7d, the RTM image shows small variation around injection zone that can not be conclusive on detection of the boundaries of $CO_2$ zones. These variations are mainly due to data residual as a result of the change in traveltime of events.

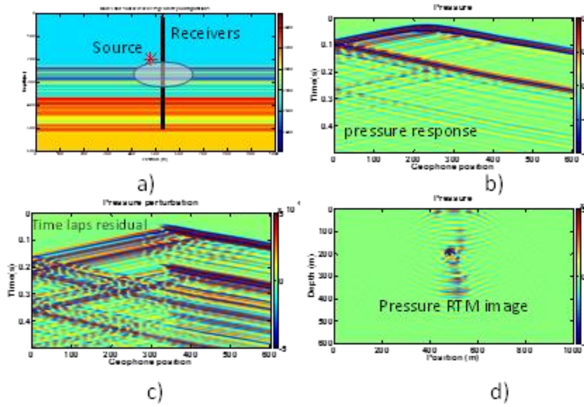


FIG.7. The cross well test for the reservoir. The first Figure is the velocity model with the injection zone and acquisition geometry. The second Figure is the pressure component of the base model (before injection) and third and fourth Figures show the difference of the seimic results (before and after injection) and Reverse Time Migration result of the pressure perturbation model.

The last example is to test effects of acquisition fold on similar problem. In Figure 8, the same background and updated model of Figure (8) is used to simulate 200 shot records of from x=200 m to x=800 m. In Figure 8b, a sample record of the pressure perturbation record is displayed. This sample is obtained from surface and VSP acquisition with sources that is positioned at the surface and interval equal 3m between shots (the blue rectangle on 8a). The RTM of all surface and VSP records are illustrated in Figure 8c and 8d respectively. Although, we increased the acquisition over the target, however, as expected both surface and VSP configurations show small amplitude of injection zone boundaries. The main contribution to the output of the images are due to the traveltime shifts that are dependant to the position of injection zone and geophone positions.  As a result, because of diffusion pattern of $CO_2$ injection, the reflection based Full Waveform migration/Inversion are not efficient compared to traveltime attributes. The next year, our field study will continue by $CO_2$ injection and seismic time lapse acquisition. Currently, all models are synthetic that will be compared with real data. The study of traveltime tomography to reduce the error in seismic time lapse monitoring is an ongoing research.

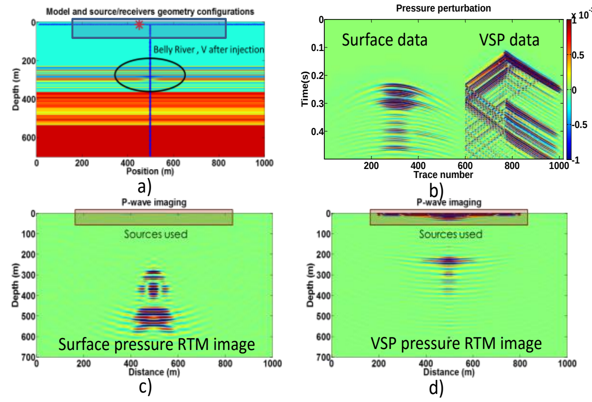


FIG.8. RTM of high fold acquisition of CO2 injection.  a) Velocity model with the injection zone and acquisition pattern the highlighted box shows source positions and the recievers are shown by blue lines located at the top and inside well position. b) A sample of the single pressure residual record at surface and VSP configuration. c) RTM of all pressure records in surface acquisition, and d)  RTM of all pressure records in VSP acquisition.

## Conclusion

We demonstrate the influence of a $CO_2$ injection model on traveltime and amplitude of seismic wavefield propagation. The effects of a $CO_2$ diffusion model on velocity and density models are estimated using fluid flow simulation. Rock physics study for the velocity and density estimation was base on the simulation results. The saturation of $CO_2$ reached to maximum 60 percent and the bulk modulus and p-wave velocity were estimated by Gassmann's equation and also the velocity demonstrates an decrease up to 4% in the core of the reservoir. In the seismic modeling different acquisition patterns such as surface, VSP and cross-well are tested for $CO_2$ imaging. We tested the difference between the blocky velocity change in the media and diffusive purturbation of $CO_2$ injection. The RTM result of data residual show high amplitude image of the blocky velocity change as compared to the ambiguous images of gas plume zones. We showed that for diffusive perturbation model of $CO_2$ injection, traveltime tomography is a better alternative as compared to the reflection migration and inversion.

## Acknowledgements

The authors thank the sponsors of CREWES for continued support and CMC Research Institutes Inc for access to the well data.  This reserach was funded by CREWES industrial sponsors and NSERC (Natural Science and Engineering Research Council of Canada) through the grant CRDPJ 461179-13.  We would like to thank Schlumberger for the use of Petrel and ECLIPSE.